# 4 Telescope and Focal Plane

### *4.1 Optical Design*

The telescope is a Ritchey-Chrétien, diffraction limited at 6.5 microns. The 85-cm diameter primary mirror and the rest of the telescope structure are fabricated entirely of beryllium, utilizing advances in optical design, testing, and fabrication to produce a lightweight telescope that operates at cryogenic temperatures. The optical design parameters for the telescope are summarized in Table 4-1 below. The telescope configuration is shown in Figure 4-1.

Note that this chapter addresses the telescope itself; the point spread function at each of the science instruments is discussed in the instrument-specific chapter (6, 7 or 8).

**TABLE 4-1**

| Optimal Parameter Description | value at 5.5 K |
|---|---|
| **System Parameters** | |
| Focal length | 10,200 mm |
| Focal ratio | f/12 |
| Back focal length (PM vertex to focus) | 437 mm |
| Field Of View (diameter) | 32.0 arcmin |
| Wavelength Coverage | 3μm - 180μm |
| **Aperture Stop** | |
| Location | Edge of primary mirror |
| Diameter of OD obscuration | 850.00 mm |
| Diameter of ID obscuration | 320.00 mm |
| Linear obscuration ratio | 0.3765 |
| **Primary Mirror (hyperbola)** | |
| Radius (concave) | -2040.00 mm |
| Conic constant | -1.003548 |
| Clear aperture | 850.00 mm |
| Focal ratio | f/1.2 |
| **Secondary Mirror (hyperbola)** | |
| Radius (convex) | -294.343 |
| Conic constant | -1.531149 |
| Clear aperture (OD) | 120.00 mm |
| PM to SM spacing (vertex to vertex) | 887.545 mm |

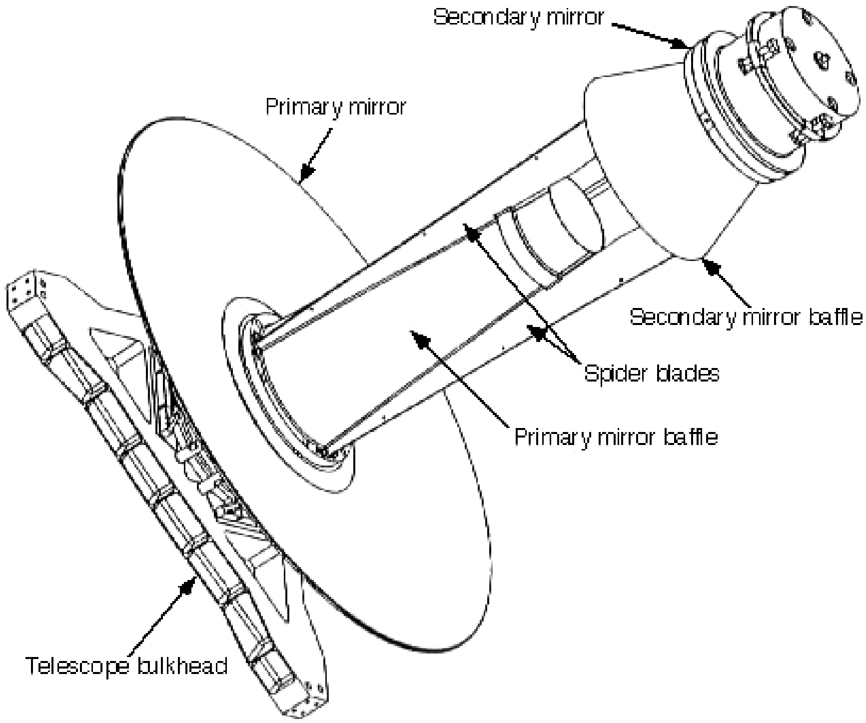


**Figure 4-1: SIRTF Telescope Assembly**

The telescope employs a single arch primary mirror, which reduces mass. The primary mirror is supported on three bipod flexures relatively close to its axis. The spider blades, primary mirror baffle, and secondary mirror baffle are integrated into a one-piece, relatively small diameter metering tower extending through the central hole in the primary mirror.

### *4.2 Optical and Thermal Performance*

#### 4.2.1 Surface Accuracy

The Ritchey-Chrétien design minimizes spherical aberration and coma over large fields of view. Field curvature varies quadratically with field angle. Similarly, the rms wave-front error at best focus varies quadratically with field angle and equals 0.52 waves ($\lambda$ = 0.6328 µm) at the edge of the field. Essentially all of this error is due to astigmatism.

The surface figure for the primary mirror was measured at cryogenic temperatures to be 0.067µm rms over the entire clear aperture, meeting the specification of 0.075µm rms (Figure 4-2).

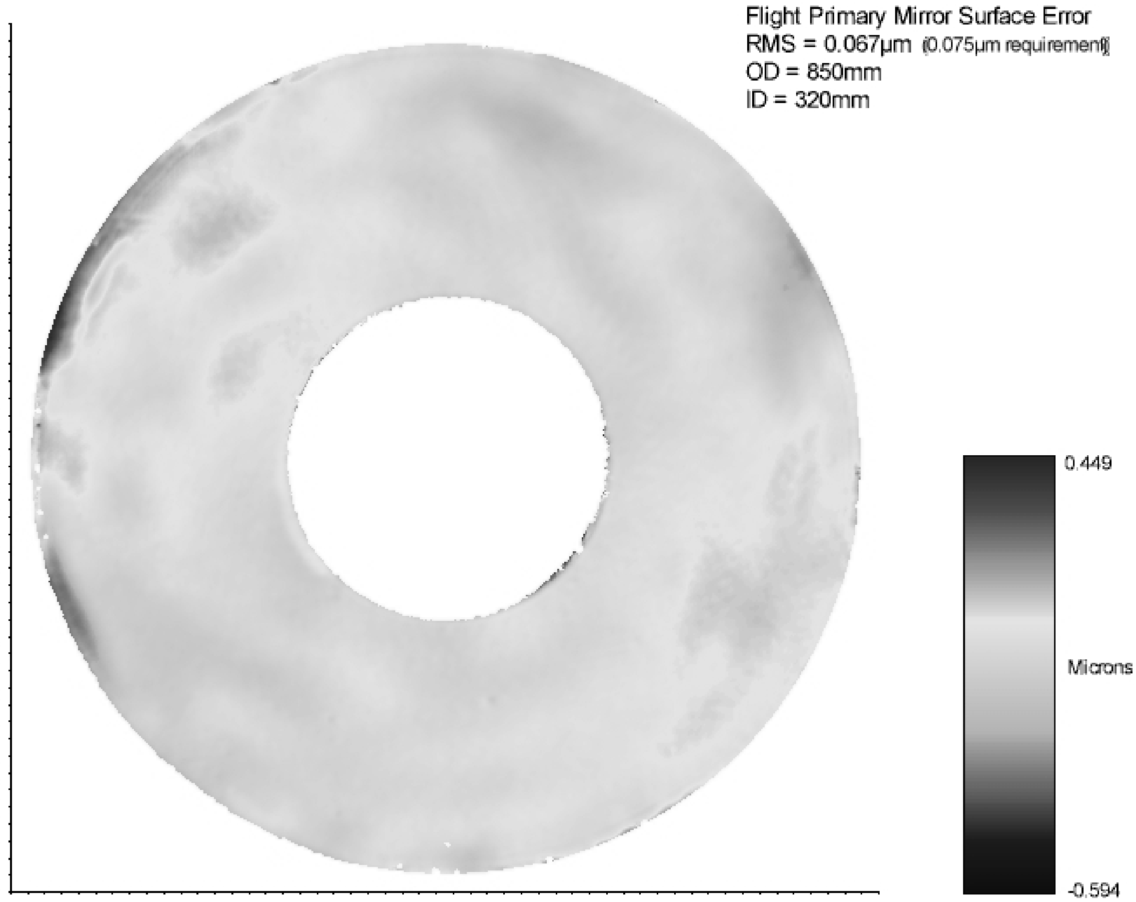


**Figure 4-2: The deviations in the flight primary mirror surface are shown. The RMS error was measured at cryogenic temperatures to be 0.067μm rms over the entire clear aperture, meeting the specification of 0.075μm rms**

### 4.2.2 Wave-front Errors

The telescope provides a beam to the telescope focal surface that is diffraction limited (transmitted wave front error $<\lambda/14$ rms) at 6.5 μm over the entire field at operating temperature. At a wavelength of 3.5 μm, the telescope produces a wave front error of less than 0.13 $\lambda$ rms over the IRAC field of view, and the image of a point source contains 45% of the encircled energy within a diameter of 2 arcseconds.

### 4.2.3 Throughput

The telescope assembly shall provide a minimum end of life throughput no less than that given in Table 4-2. Telescope throughput is defined as the ratio of energy from a point source reaching the telescope focal surface to the energy collected by an 85 cm diameter mirror. Factors that degrade telescope throughput are the central obscuration (including spiders), mirror reflectivity as a function of wavelength and losses due to contamination.

**Table 4-2: Telescope Throughput**

| Wavelength (μm) | End of Life Throughput |
|---|---|
| 0.55 | > 0.18 |
| 3.5–6.5 | > 0.70 |
| 6.5–10 | > 0.73 |
| 10–20 | > 0.74 |
| 20–200 | > 0.75 |

### 4.2.4 Stray Light Rejection

The cryostat, telescope, multiple instrument chamber and science instruments are designed and baffled such that, at all wavelengths from 3.6 μm to 160 μm, celestial stray radiation and internal stray radiation:

- Do not, except for lines of sight near bright sources, increase by more than 10% the photon noise of the natural background in the direction of the line of sight of the telescope. This requirement implies that the combination of celestial stray radiation and internal stray radiation must be <21% of the natural background at the instrument detector arrays.
- Display no gradients or glints in the celestial stray light that will increase confusion noise over natural levels or produce false sources.
- Do not significantly decrease the contrast of the first dark ring of the diffraction limited point spread function.

The conformance of the SIRTF design to its stray light requirements was verified by analysis using the APART stray light analysis program and an analytical test source designed to approximate the brightest celestial source expected in each of SIRTF's wavelength bands. The actual scattered light performance of the SIRTF Observatory will be characterized on orbit during In-Orbit Checkout and during nominal operation of the Observatory.

A useful output from the analysis is a set of predicted point source transmission curves. The point source transmission function (PST) relates the flux density (W/m$^2$/Hz) of an off axis source to the flux density at the telescope focal plane due to light scattered from that source. The separate PST curves in Figure 4-3 refer to different azimuthal locations of the celestial point source. An azimuth of 0 degrees refers to the anti-Sun direction. The differences among the azimuths are mainly due to the changing illumination of struts supporting the secondary mirror. Figure 4-4 shows the variation as a function of wavelength.

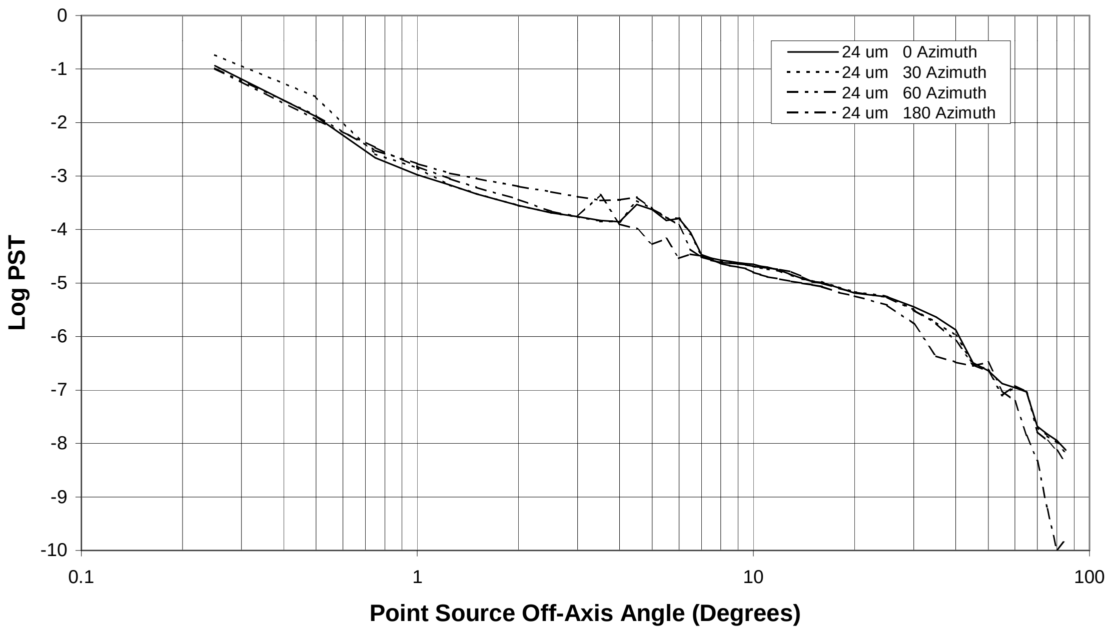


**Figure 4-3: PST for 24 microns off-axis as a function of azimuth.**

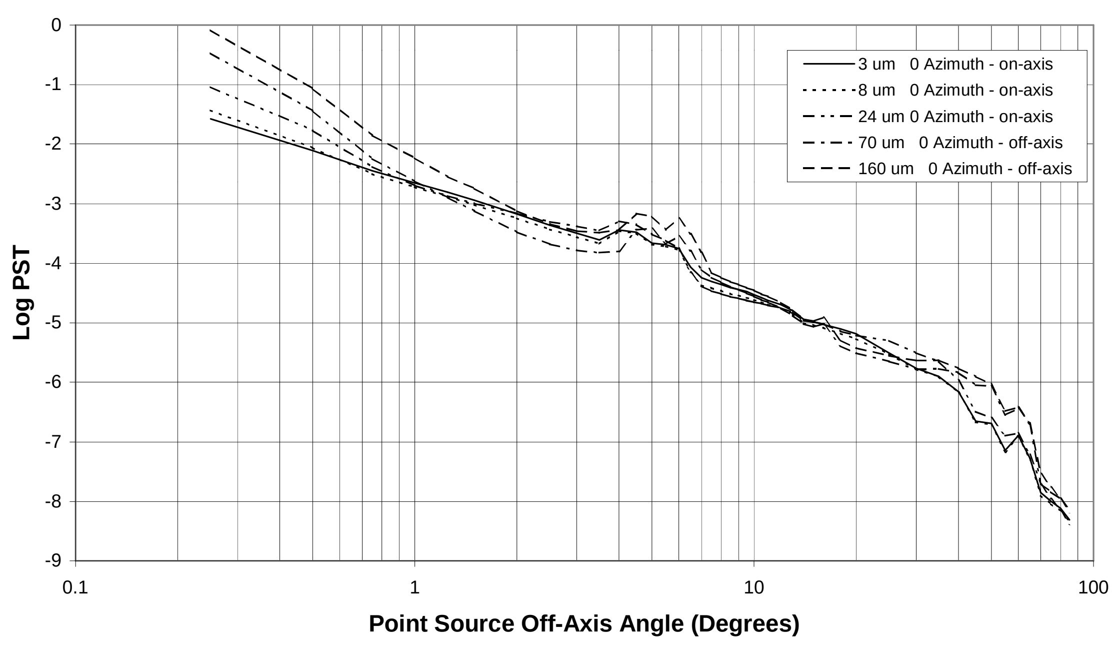


**Figure 4-4: PST as function of wavelength for fixed azimuth on-axis.**

These plots can be used to estimate the stray light contribution from a given source. For example, at 8 μm Vega has a flux density of ~62 Jy. From Figure 4-4, the 8 μm PST at 1 degree off axis is $\sim 2\times 10^{-3}$, so the predicted flux density in the SIRTF focal plane due to Vega at 1 degree off axis is 120 mJy.[12]

### 4.2.5 Telescope Temperature/Thermal Background.

The telescope is cooled by helium vapor vented from the cryostat. The helium vaporization is driven by power dissipated by the Science Instrument cold assemblies. A supplemental heater is available to drive additional vaporization, if needed. The required telescope temperature and heat load set the required helium flow rate. As discussed in Section 3.1.1, the telescope will be launched warm and will gradually be cooled by a combination of radiative cooling and helium boil-off to ≤5.5K during the first 30 days in orbit. Following the initial cool-down, the telescope temperature will vary between (<5.5K and 12K) depending upon how much power is dissipated in the cryostat. The power thus dissipated depends primarily upon the science instrument in use; the "make-up" heater may be used to ensure that the telescope is maintained at 5.5 K when needed for 160-micron observations.

### 4.2.6 Telescope Focus

SIRTF is equipped with a focus mechanism, which can be operated both on the ground and on orbit. The end-to-end image quality will be measured on the ground and the mechanism will be set to the position that is predicted to give optimal focus following on-orbit cool-down. During In-Orbit Checkout (IOC), it will be confirmed that the telescope is in focus, and the focus can be adjusted during IOC if necessary. The instruments are designed to be confocal so that separate adjustment of the focus for each instrument will not be necessary.

## *4.3 Focal Plane Layout*

Figure 4-5 shows the actual location of the pick-off mirrors that feed the science instruments as if viewed from above (looking down the boresight). The Y- and Z-axis directions are the same as the Observatory coordinate system described in Chapter 3. Figure 2-1 shows the SIRTF entrance apertures as projected onto the sky and appears inverted compared to Figure 4-5 due to the combined

---

[12] The natural background at 8 μm near an ecliptic pole is 5.3 MJy/sr, which is imaged to a flux density of $5.3\ \mathrm{MJy/sr} \times \pi/(4\times 12^2) = 2.9\times 10^4$ Jy in the focal plane of the f/12 SIRTF telescope. The scattered light from Vega at 1 degree off axis is far below the natural background. The first stray light trouble from Vega at 8 μm should come from the outer parts of its diffraction limited point spread function.

effects of looking out from behind the focal plane and the projection of the sky onto the focal plane through the telescope optics.

**SIRTF Nominal Aperture or Pick-Off Mirror Locations Viewed Down the Telescope**

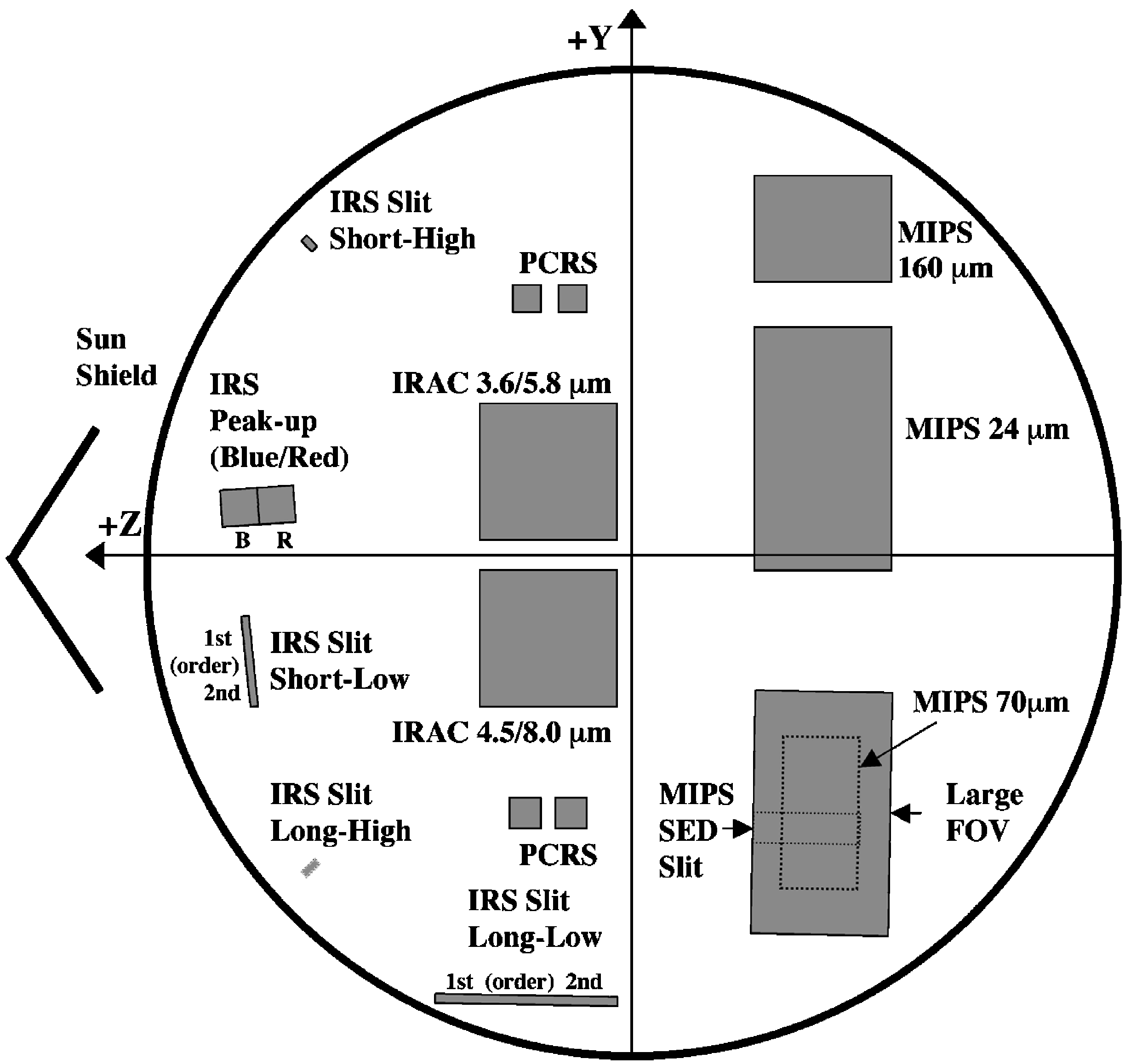


**Nominal Field Radius = 16 arcminutes**

Note: This is an approximate mechanical layout of the focal plane as viewed from above. It is not a projection onto the sky.

**Figure 4-5: Schematic view SIRTF Focal Plane from above, looking down the boresight. The solar panel is on the IRS side of the spacecraft. This figure shows the region of the focal surface where the pick-off mirrors for each instrument are located. This is in contrast to where the apertures project onto the sky. See Figure 2-1 for comparison.**